THE JOURNAL OF PHYSICAL CHEMISTRY C

Article

pubs.acs.org/JPCC

Simple and Accurate Method for Time-Dependent Transport along Nanoscale Junctions

Liping Chen,[†] Thorsten Hansen,[‡] and Ignacio Franco*,[†]

[†]Department of Chemistry and The Center for Coherence and Quantum Optics, University of Rochester, Rochester, New York 14627, United States

[‡]Department of Chemistry, H.C. Ørsted Institute, University of Copenhagen, DK 2100 Copenhagen Ø, Denmark

ABSTRACT: A simple method that accurately captures the dynamics of metal−molecule−metal junctions under the influence of time-dependent driving forces is presented. In the method, the metallic contacts are modeled explicitly as a discrete set of levels that are dynamically broadened via an artificial damping term in the equations of motion. The approximations that underlie the method are revealed via a derivation of the effective equations of motion within the framework of nonequilibrium Green's functions (NEGF) theory. As shown, the method applies to junctions that can be described by an effective independent Fermion Hamiltonian, admits arbitrary time dependence in the molecular Hamiltonian, and is restricted to time-dependent voltages that are adiabatically slow. The method is trivial to implement computationally, has a well-defined range where the results are independent of artificial model parameters, and is numerically shown to quantitatively reproduce the time-dependent transport characteristics of a model molecular junction driven by laser fields as described by an exact NEGF method in the wide band limit. As such, it generalizes previous efforts to capture Landauer transport via effective Liouville equations of motion with damping terms and constitutes an intuitive and technically accessible method for modeling time-dependent transport phenomena in molecular junctions that are driven by electric fields or fluctuating environments.

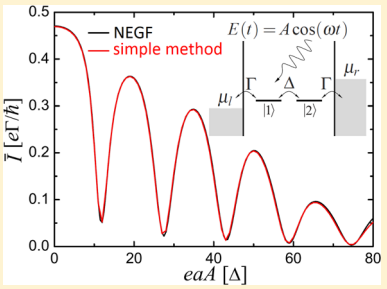

1. INTRODUCTION

Considerable effort has been devoted to the development of theoretical methods that are useful in the description of charge transport along metal−molecule−metal junctions.[1−4] The focus has traditionally been placed on capturing the steady-state current induced by an applied voltage where the scattering-based Landauer−Büttiker formalism provides a useful starting point for more sophisticated approaches.[5,6] A more recent area of focus has been the development of explicitly time-dependent formulations for the transport that capture transient behavior or transport under circumstances where no steady-state solution exists.[7−15] The latter occurs, for example, when the junction is subject to a laser field, to a time-dependent voltage, or to interaction with a fluctuating environment.

In its most basic form, the theoretical description of time-dependent charge transport along a nanojunction is a problem in open quantum system dynamics where the molecular system exchanges particles and energy with the metallic contacts. Approaches to describe time-dependent transport include master equations techniques,[9,16,17] open-boundary schemes within time-dependent density functional theory (TDDFT),[8] non-equilibrium Green's function methods (NEGF),[7,12] schemes that combine TDDFT and NEGF with the hierarchical equation of motion approach to open quantum dynamics,[10,13−15] hybrid Floquet−NEGF treatments,[18,19] and the multilayer multi-configuration time-dependent Hartree theory.[20,21]

While the push in the field has naturally been toward developing methodologies of increased generality and sophistication, our objective here is quite different. The question that we ask is: what is the simplest possible way to quantitatively describe time-dependent transport along a nanoscale junction? Aside from convenience in computation, simple methods often shed light on the essential elements required in the physical description of a problem.

A glimpse into how a simple methodology might be developed in this case follows from the recent observations[22−25] that the Landauer current (and the nonequilibrium steady-state populations[23]) can be reproduced by determining the steady-state solution for the reduced density matrix of a molecule attached to a finite segment of leads with damping terms in the equations of motion that enforce open-boundary conditions.

In this paper, we investigate the possible use of the simple equations of motion heuristically derived in ref 25 to follow transient behavior in nanojunctions with time-dependent Hamiltonians. For time-independent Hamiltonians, these equations of motion are known to reproduce Landauer transport in the steady state.[25] However, because a rigorous derivation of the equations of motion is lacking and no numerical comparison with exact time-dependent transport results has been presented, it is unclear if this approach can successfully capture transient or time-dependent transport behavior.

Received: June 10, 2014
Revised: July 31, 2014
Published: August 4, 2014

We show that, quite remarkably, this simple set of equations is also capable of accurately reproducing the time-dependent transport characteristics of a molecular wire even under rather extreme driving conditions. As a particular time-dependent realization, we focus on photoinduced transport;[26] more specifically, on laser-induced symmetry breaking[27−32] and on the coherent destruction of tunneling.[9,33−36] The results are benchmarked against Lodestar, which is a state-of-the-art NEGF time-dependent transport code based on the developments summarized in ref 15. To unveil the approximations that underlie the method, the effective equations of motion are derived from NEGF transport theory. As shown, the method is applicable to any system with an effective independent electron Hamiltonian such as that produced by TDDFT and allows for arbitrary temperature, molecule−lead coupling, and driving forces on the molecule. The time-dependence in the voltage can be captured at the adiabatic level where it is supposed that changes in the voltage do not lead to excitations in the metallic contacts.

The structure of this paper is as follows: In Section 2 the phenomenological equations and parameters proposed to model the time-dependent transport across molecular junctions are introduced. Sections 3.1 and 3.2 illustrate the ability of the method to accurately capture asymptotic and transient currents using a laser- and voltage-driven two-level molecule as an example. Section 3.3 identifies a well-defined range where the results are independent of fictitious model parameters. In turn, Section 3.4 presents a derivation of the equations of motion within the framework of NEGFs. Our main results are summarized in Section 4.

2. MODEL AND METHODS

The Hamiltonian for a time-dependent metal−molecule−metal junction is given by

$$H(t) = H_{\mathrm{M}}(t) + H_{\mathrm{L}}(t) + H_{\mathrm{ML}}(t) \tag{1}$$

where $H_{\mathrm{M}}(t)$ describes the molecule, $H_{\mathrm{L}}(t)$ the leads, and $H_{\mathrm{ML}}(t)$ the molecule−lead coupling. Here it is supposed that $H(t)$ is an effective single-particle Hamiltonian such as that expected from TDDFT. In this case, the device region can be expressed as

$$H_{\mathrm{M}}(t) = \sum_{n} \varepsilon_n(t) c_n^{\dagger} c_n + \sum_{n \neq m} V_{nm}(t) c_n^{\dagger} c_m \tag{2}$$

where the operator $c_n^{\dagger}$ (or c_n) creates (or annihilates) a Fermion in a single-particle level n of energy $\varepsilon_n(t)$. Such levels may be coupled to one another through $V_{nm}(t)$. The leads are described by

$$H_{\mathrm{L}}(t) = \sum_{\beta=\mathrm{l,r}} \sum_{q} \varepsilon_{\beta q}(t) c_{\beta q}^{\dagger} c_{\beta q} \tag{3}$$

where $c_{\beta q}^{\dagger}$ and $c_{\beta q}$ are the Fermionic operators for the lead states and $\beta = \mathrm{l}$ or r denotes the left or right lead, respectively. Last, the molecule−lead coupling is given by

$$H_{\mathrm{ML}}(t) = \sum_{\beta=\mathrm{l,r}} \sum_{n,q} V_{nq}^{\beta}(t) c_{\beta q}^{\dagger} c_n + \mathrm{H.c.} \tag{4}$$

where $V_{nq}^{\beta}(t)$ are the couplings between the molecule and lead β, and H.c. denotes Hermitian conjugate. The effective molecule−lead coupling is specified by the spectral density

$$\Gamma_{n,\beta}(\varepsilon, t) = 2\pi \sum_{q} |V_{nq}^{\beta}(t)|^2 \delta(\varepsilon - \varepsilon_{\beta q}) \tag{5}$$

a quantity that contains information about the characteristic frequencies of the leads and their coupling to the molecule. Because the Hamiltonian in eq 1 is a single-particle operator, all electronic properties of the composite system are determined by the single-particle reduced density matrix

$$\rho_{uv}(t) = \langle c_v^{\dagger} c_u \rangle \tag{6}$$

where the labels in the Fermionic operators can refer to molecular or lead levels. The dynamics of such reduced density matrix is determined by the single-particle Liouville's equation of motion

$$\frac{\mathrm{d}\rho}{\mathrm{d}t} = -\frac{\mathrm{i}}{\hbar}[H, \rho] \tag{7}$$

In what follows, we focus on the wide-band limit (WBL) where the $V_{nq}^{\beta}(t)$ and the leads' density of states $\eta = \sum_q \delta(\varepsilon - \varepsilon_{\beta q})$ are assumed to be energy independent. In this case, the $\Gamma_{n,\beta}(\varepsilon,t)$ is also energy independent and given by $\Gamma_{n,\beta}(t) = 2\pi\eta|V_n^{\beta}(t)|^2$. Note, however, that the method described below can in principle operate beyond the WBL provided the molecule−lead couplings in eq 4 are known. These couplings can be calculated, for example, by determining the eigenstates of the composite system in site representation and then employing site-to-state unitary transformations as exemplified in ref 25.

Generally, if one attempted to integrate eq 7 directly, an infinite number of states would be required to describe the continuum electronic structure of the macroscopic leads. In principle, as shown in Figure 1, that continuum can be numerically discretized into a finite N_q number of states in the $[E_{\min}, E_{\max}]$ energy range equidistantly spaced at $\Delta\varepsilon_q$ intervals. However, the resulting structure will not, in general, behave like a continuum. To make the finite set of levels behave like a continuum, as was done previously for steady-state transport,[22,23,25] the equations of motion are supplemented with a fictitious damping term that effectively broadens the lead levels. Specifically, eq 7 is now expressed as

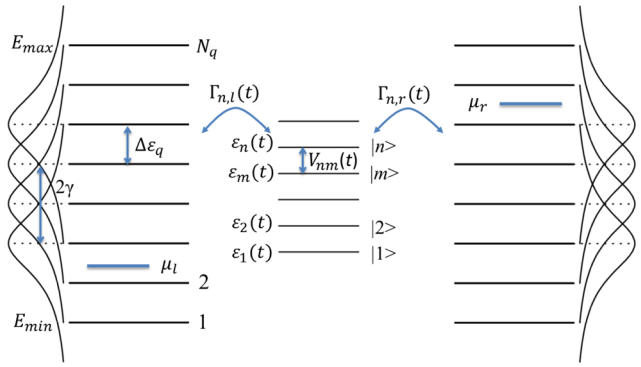

Figure 1. Scheme of the model used to describe driven molecular junctions. The molecule consists of a series of levels $|n\rangle$ with energies $\varepsilon_n(t)$ that are coupled via $V_{nm}(t)$. The molecule is coupled to the leads through $\Gamma_{n,\mathrm{l}}(t)$ and $\Gamma_{n,\mathrm{r}}(t)$. The leads (with Fermi energies μ_{l} and μ_{r}) are described by a finite number of states N_q equidistantly spaced every $\Delta\varepsilon_q$ in the $[E_{\min}, E_{\max}]$ energy range. The damping term in eq 8 introduces Lorentzian broadening to the leads' levels with full width at half-maximum of 2γ. For $2\gamma \geq \Delta\varepsilon_q$, the set of levels representing the leads effectively behave like a continuum.

$$\dot{\rho} = -\frac{\mathrm{i}}{\hbar}\left[\begin{pmatrix} H_{\mathrm{M}}(t) & H_{\mathrm{ML}}(t) \\ H_{\mathrm{ML}}(t) & H_{\mathrm{L}}(t) \end{pmatrix}, \begin{pmatrix} \rho_{\mathrm{M}} & \rho_{\mathrm{ML}} \\ \rho_{\mathrm{LM}} & \rho_{\mathrm{L}} \end{pmatrix}\right] - \frac{\gamma}{\hbar}\begin{pmatrix} 0 & 0 \\ 0 & \rho_{\mathrm{L}} - \rho_{\mathrm{L}}^{\mathrm{eq}} \end{pmatrix} - \frac{\gamma}{2\hbar}\begin{pmatrix} 0 & \rho_{\mathrm{ML}} \\ \rho_{\mathrm{LM}} & 0 \end{pmatrix} \tag{8}$$

Here, the single-particle density matrix has been split into a molecular part ρ_{M}, a lead part ρ_{L}, and the molecule−lead coherences ρ_{ML} (where $\rho_{\mathrm{ML}} = \rho_{\mathrm{LM}}^{*}$). In general, ρ_{L} contains coherences between the two leads. The second term on the right-hand side (RHS) of eq 8 dynamically forces the leads' density matrix to decay to a thermal distribution $\rho_{\mathrm{L}}^{\mathrm{eq}}$ at a rate determined by $\gamma/\hbar$. As pointed out in ref 25, the third term on the RHS of eq 8 where the molecule−lead coherences are damped at a rate of $\gamma/2\hbar$ is necessary to preserve Pauli's exclusion principle and the positivity of the diagonal of the density matrix. In thermal equilibrium there are no coherences between leads, and the density matrix of each lead is described by the Fermi−Dirac distribution with matrix elements

$$\rho_{qq'}^{\mathrm{eq},\beta} = \delta_{qq'}\frac{1}{1 + \exp[(\varepsilon_{\beta q} - \mu_\beta)/k_{\mathrm{B}}T]} = f_\beta(\varepsilon_{\beta q}) \tag{9}$$

where μ_β is the chemical potential for lead β and T the temperature. For each lead level, the net effect of γ is to introduce Lorentzian broadening with full width at half-maximum (fwhm) of 2γ. This is consistent with previous developments[37] that fit the leads' self-energy as a sum of discrete Lorentzian functions. As shown in Section 3.3, the discretized lead states essentially behave like a continuum when $2\gamma \geq \Delta\varepsilon_q$.

Last, the current entering lead β is given by

$$I_\beta(t) = -e\frac{\mathrm{d}}{\mathrm{d}t}\left(\sum_q \langle c_{\beta q}^\dagger c_{\beta q}\rangle\right) = -e\frac{\mathrm{i}}{\hbar}\langle[H(t), \sum_q c_{\beta q}^\dagger c_{\beta q}]\rangle = -\frac{2e}{\hbar}\sum_{n,q} V_{nq}^\beta(t)\mathrm{Im}(\langle c_{\beta q}^\dagger c_n\rangle) \tag{10}$$

where e is the elementary charge of an electron. The net current passing through the nanojunction is calculated as the average current flowing into the two leads

$$I(t) = (I_{\mathrm{l}}(t) - I_{\mathrm{r}}(t))/2. \tag{11}$$

In the steady state or for nontransient processes, $I_{\mathrm{l}} + I_{\mathrm{r}} = 0$.

A scheme of the resulting model proposed to describe the junction is shown in Figure 1. The accompanying equations of motion, eqs 8 and 10, constitute a set of coupled linear differential equations that are straightforward to integrate using, for example, a Runge−Kutta method of order 4; this is the strategy that we adopt. These and closely related equations have numerically been shown to reproduce the steady-state Landauer transport.[22−25] Below, we numerically demonstrate that they can also quantitatively capture time-dependent phenomena in junctions and isolate a well-defined range where results are independent of fictitious model parameters $[E_{\mathrm{min}}, E_{\mathrm{max}}]$, γ and $\Delta\varepsilon_q$. This is done by comparing results obtained using eqs 8 and 10 with those generated by an essentially exact state-of-the-art finite temperature NEGF method[15] that uses the WBL and a Padé expansion[38] for the Fermi−Dirac distribution. Importantly, via explicit derivation of the equations of motion, we also provide a connection with NEGF transport theory and isolate the approximations underlying the method.

3. RESULTS AND DISCUSSION

For definitiveness, to test the theoretical ansatz in eq 8 we focus on laser-driven transport in which the time dependence in the Hamiltonian arises because of laser−matter interactions. As a specific model, we consider a two-site tight-binding molecule interacting with a laser field $E(t)$ in dipole approximation with Hamiltonian

$$H_{\mathrm{M}}(t) = \sum_{n=1}^{2}\varepsilon_n c_n^\dagger c_n - \Delta(c_1^\dagger c_2 + c_2^\dagger c_1) + \frac{eaE(t)}{2}(c_1^\dagger c_1 - c_2^\dagger c_2) \tag{12}$$

where $c_n^\dagger$ (c_n) creates (annihilates) an electron at site n with onsite energy ε_n and a is the length between sites. Both sites are coupled via a tight-binding parameter Δ. For $\varepsilon_1 = \varepsilon_2$, the eigenlevels of the isolated molecule are separated by an energy gap 2Δ. The molecule−lead interaction term H_{ML} is taken to be

$$H_{\mathrm{ML}}(t) = \sum_q (V_{\mathrm{l}q}(t)c_{\mathrm{l}q}^\dagger c_1 + V_{\mathrm{r}q}(t)c_{\mathrm{r}q}^\dagger c_2) + \mathrm{H.c.} \tag{13}$$

such that site 1 couples to the left lead and site 2 to the right lead. Throughout we suppose the coupling to either lead to be identical and given by $\Gamma = \Gamma_\beta = 2\pi\eta|V_\beta(t)|^2$.

We focus on the description of two well-known laser-driven phenomena in junctions: the coherent destruction of tunneling[9,33−36] (in which a properly designed continuous wave laser field can drive coherent tunneling to an almost complete standstill) and laser-induced symmetry breaking[27−32] (in which laser fields with frequency components ω and 2ω induce phase controllable currents in spatially symmetric systems). Such phenomena can operate under perturbative and nonpertubative driving conditions and are sensitive to the continuum structure of the leads, providing a useful testing ground for the methodology.

3.1. Asymptotic Currents. Consider first the ability of eq 8 to accurately describe asymptotic time-dependent currents across a junction. Figure 2 shows the time-averaged current $\bar{I}$ induced by a bias voltage under the influence of a nonresonant continuous wave laser field of the form $E(t) = A\cos(\omega t)$ of varying amplitude. This type of laser-modulation of transport has been described in detail elsewhere (see, e.g., ref 39). As shown, the laser modulates the tunneling current and for specific laser

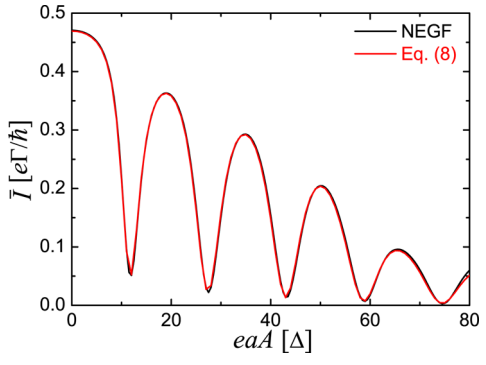

Figure 2. Coherent destruction of tunneling as described by eq 8 and a NEGF method. The plot shows the asymptotic time-averaged current $\bar{I}$ induced by a bias voltage and modulated by a laser field $E(t) = A\cos(\omega t)$ as a function of the laser driving amplitude A for a two-level molecular junction with energy gap 2Δ. Here, $\hbar\omega = 5\Delta$, $\varepsilon_1 = \varepsilon_2 = 0$, $-\mu_{\mathrm{l}} = \mu_{\mathrm{r}} = 24\Delta$, $\Gamma = 0.5\Delta$, and $k_{\mathrm{B}}T = 0.1\Delta$. In solving eq 8 we used $\gamma = 0.3\Delta$, $N_q = 500$ and $\Delta\varepsilon_q = 0.2\Delta$. Note the agreement between the two methods even under extreme driving conditions.

dx.doi.org/10.1021/jp505771f | J. Phys. Chem. C 2014, 118, 20009−20017

parameters ($eaA/\hbar\omega$ = 2.405, 5.520, 8.654, and so on[39]) essentially quenches the transport. This is the so-called coherent destruction of tunneling. For the present purposes what is important to note is that in the absence of a laser field and for weak and strong driving conditions the results obtained using eq 8 accurately reproduce those generated by the exact NEGF transport formalism. Furthermore, the observed asymptotic currents were found to be independent of how fast the molecule–lead coupling in eq 13 is turned on.

As a second test, we consider the case in which there is no bias voltage, the junction is spatially symmetric, and a laser field $E(t) = A_\omega \sin(\omega t) + A_{2\omega} \sin(2\omega t + \phi)$ with ω and 2ω frequency components is used to break the spatial symmetry of the system and generate a current. To third order in the field, such lasers are known to generate net phase controllable currents of the form $I \propto A_\omega^2 A_{2\omega} \cos(\phi + \alpha)$ where ϕ is the relative phase between the ω and 2ω components and α is the molecular phase.[27] The molecular phase is sensitive to the continuum structure of the junction and is a quantum signature of the particular bound-to-continuum transitions exploited for the generation of transport.[27,40,41] Figure 3 shows the asymptotic time-averaged photoinduced current when the 2ω component is chosen to be at resonance (laser and junction parameters are specified in the figure) as a function of the relative phase ϕ for two different molecule–lead coupling strengths $\Gamma = 0.01\Delta$ and 0.10Δ. The figure shows the usual sinusoidal control map for this coherent control scenario under conditions previously detailed in ref 31. As in the previous example, the results obtained with eq 8 accurately reproduce the NEGF results, including the magnitude of the current and its dependence on the relative laser phase. Note that, quite importantly, eq 8 also correctly captures the molecular phase determining the phase lag of the control map. Such molecular phase is known to sensitively depend on the continuum structure;[40,41] hence, this is a strong indication that the broadening procedure in eq 8 reproduces such structure correctly.[42]

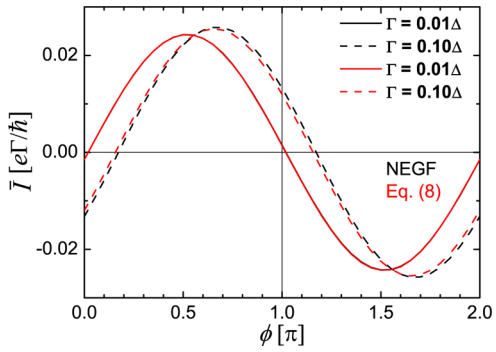

Figure 3. Laser-induced symmetry breaking as described by eq 8 and a NEGF method. The plot shows the asymptotic time-averaged current $\bar{I}$ induced by a laser field $E(t) = A_\omega \sin(\omega t) + A_{2\omega} \sin(2\omega t + \phi)$ as a function of the relative phase ϕ for a two-level molecular junction with the Hamiltonian in eqs 12 and 13. Here, $eaA_\omega = 2eaA_{2\omega} = \Delta$, $\hbar\omega = \Delta$, $\varepsilon_1 = \varepsilon_2 = 0$, $\mu_l = \mu_r = 0$, and $k_BT = 0.25\Delta$. Equation 8 correctly captures the magnitude and phase dependence of the control.

We have also performed computations using a longer 10-site molecule as an example (not shown) which exhibited equally good agreement between results obtained using eq 8 and those obtained using the NEGF method in ref 15.

3.2. Transient Behavior. As an additional important test we now show that eq 8 can also correctly describe transient junction behavior. To do so we investigate how a 400 fs Gaussian pulse modulates the steady-state transport induced by a bias voltage. As in ref 35, the laser parameters are chosen such that the laser is expected to suppress transport via coherent destruction of tunneling. Specifically, at maximum laser intensity $eaA/\hbar\omega$ is 2.405, which corresponds to the first current dip in Figure 2. The evolution of the transient current is shown in Figure 4. The system begins in a steady-state situation where a bias voltage induces a current across the junction. As the laser field develops, the average current (blue lines) decays, with tunneling transport essentially being suppressed at the center of the pulse. As the laser field fades, the average current increases gradually. Finally, it is reestablished completely. Note that results obtained using eq 8 coincide with those of the NEGF method, indicating that the simple method accurately describes transient behavior too. Nevertheless, because in this method the leads are considered explicitly, it is computationally less efficient than the NEGF method where the leads are considered implicitly. For instance, the results in Figure 4 require 5 CPU hours on an Intel Xeon 2.7 GHz processor, whereas Lodestar requires 0.2 h in the same processor.

3.3. Applicable Range of Parameters. Having exemplified the versatility and accuracy of the method, it is now important to discuss the parameter range in which the method is applicable. The parameters to be considered (recall Figure 1) are (1) the

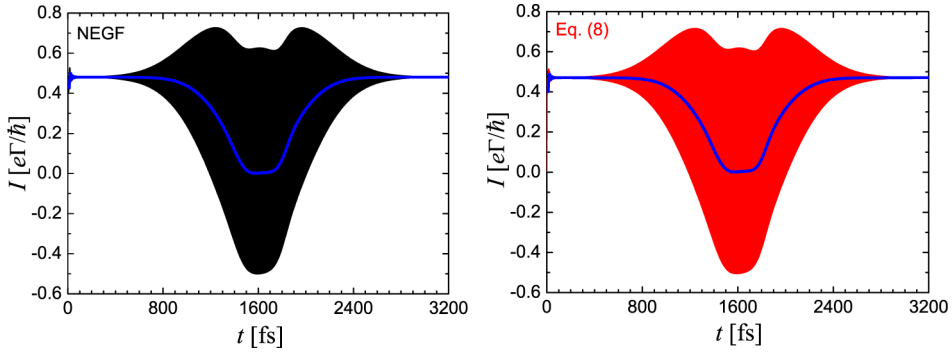

Figure 4. Transient modulation of a steady-state current by a 400 fs Gaussian laser pulse as computed with eq 8 and a NEGF method for a two-level molecular junction defined by the Hamiltonian in eqs 12 and 13. Here, $\varepsilon_1 = \varepsilon_2 = 5\Delta$, $\mu_l = 10\Delta$, $\mu_r = 0$, $\Gamma = 0.4\Delta$, and $k_BT = 0.25\Delta$. The laser pulse $E(t) = A \exp[-(t - T_0)^2/(2\sigma^2)] \sin(\omega t)$ is centered at T_0 = 1600 fs, with a width σ = 400 fs and central frequency $\hbar\omega = 10\Delta$. The quantity $eaA/\hbar\omega = 2.405$ is chosen such that the laser suppresses transport through coherent destruction of tunneling. Blue lines indicate the time-dependent averaged current over three periods of the laser field. Note that eq 8 accurately captures the transient and asymptotic transport characteristics of the time-dependent junction.

dx.doi.org/10.1021/jp505771f | J. Phys. Chem. C 2014, 118, 20009–20017

energy range $[E_{min}, E_{max}]$ for the leads (we use $-E_{min} = E_{max} = E$), (2) the number of states in the leads N_q, and (3) the damping parameter γ in eq 8. Note that the parameters used to describe the leads (E, N_q, $\Delta\varepsilon_q$, and η) are related through $\Delta\varepsilon_q = 1/\eta = 2E/N_q$.

To test parameter dependence, we focus on the laser-induced currents described in Figure 3 with $\Gamma = 0.10\Delta$ and $\phi = 0.65\pi$, which corresponds to a maximum in the control map. The asymptotic time-averaged current resulting from eq 8 using different values for E, N_q and γ (with other parameters kept constant) are shown in Figure 5. Figure 5a shows the dependence of the asymptotic current on the energy bandwidth of the leads. For bandwidths smaller or comparable to the spread in energy of molecular levels (in this case 2Δ) the method gives inaccurate results. However, once all molecular levels are contained within the leads' energy bandwidth, the current quickly converges with increasing E. In what follows we choose $E = 5\Delta$ because it provides well-converged results for the model considered.

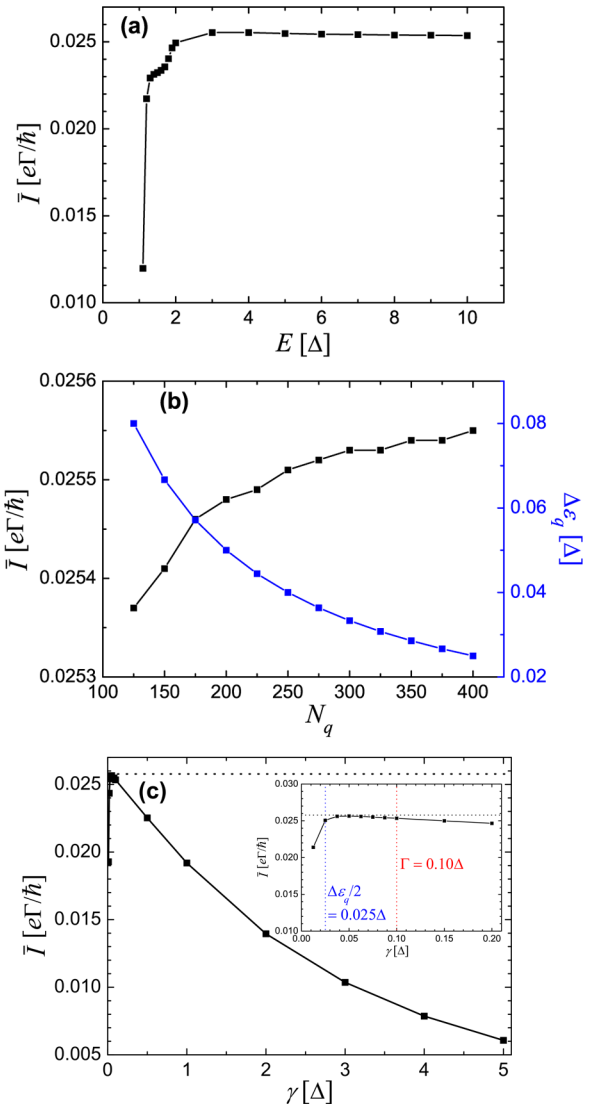

Figure 5. Dependence of the results obtained with eq 8 on the fictitious parameters employed to describe the leads. The plots show the time-averaged asymptotic current induced by a laser field as described in Figure 3 with $\Gamma = 0.10\Delta$ and $\phi = 0.65\pi$ as a function of (a) half bandwidth E of the leads with $\Delta\varepsilon_q = 0.05\Delta$ and $\gamma = 0.08\Delta$, (b) number of lead states N_q with $E = 5\Delta$ and $\gamma = 0.08\Delta$, and (c) damping parameter γ with $E = 5\Delta$ and $N_q = 200$. The black dotted line indicates the NEGF result.

Figure 5b shows the dependence of the current on the number of lead levels N_q (or, equivalently, on the level spacing between lead levels $\Delta\varepsilon_q$) for fixed E. As shown, beyond a certain threshold value for N_q (or $\Delta\varepsilon_q$) the current is essentially unchanged by increasing N_q (or decreasing $\Delta\varepsilon_q$). The origin of such a threshold is best revealed by studying the dependence of the currents on the decay parameter γ. This is shown in Figure 5c for $E = 5\Delta$ and $N_q = 200$ (or $\Delta\varepsilon_q = 0.05\Delta$). From a spectral perspective, the effect of γ is to dynamically broaden the lead levels into Lorentzians with fwhm of 2γ. Thus, for $2\gamma < \Delta\varepsilon_q$ the set of lead levels are spectrally isolated and the finiteness of the Hilbert space of the model of the leads manifests as a reduction in the net observed current. By contrast, for $2\gamma \geq \Delta\varepsilon_q$ the lead levels are no longer spectrally isolated and for all practical purposes represent a continuum. Nevertheless, if γ is too large the current drops dramatically and goes almost to 0. In fact, when $\gamma \gg \Gamma$ the dynamics cannot capture processes to all orders in the physical Γ before excitations are quenched by the γ-induced population decay in the leads. As shown in the inset of Figure 5c, γ is best chosen such that $\Gamma > \gamma \geq \Delta\varepsilon_q/2$. In this range, the results are largely insensitive to the fictitious model parameters and coincide with the NEGF results in the WBL. A similar applicable range of model parameters was observed in the steady-state case when employing equations of motion reminiscent of eq 8 but that do not take into account the decay of molecule−lead coherences.[23]

3.4. Derivation within the Framework of NEGF. To understand why the simple eq 8 is successful in capturing time-dependent transport, we now derive it using the formalism of NEGF. In essence, we seek an equation of motion of the form

$$\dot{\rho} = -\frac{i}{\hbar}[H, \rho] - \frac{\gamma}{\hbar}(Q\rho Q - Z) - \frac{\gamma}{2\hbar}(Q\rho P + P\rho Q) \tag{14}$$

where Z is a positive semidefinite matrix and H is the noninteracting Hamiltonian for the junction as in eq 1; P and Q are operators that project onto the molecule and explicit lead subspaces, respectively. Throughout, we refer to the junction as the molecule plus the segment of the leads that is considered explicitly in the simulations. To capture the damping terms in the equations of motion, the explicit lead levels in the junction are connected to an even larger Fermionic reservoir with Hamiltonian $\mathcal{H}_B$ and reservoir-lead couplings $\mathcal{W}$. The total Hamiltonian of the reservoir-junction-reservoir tripartite system is

$$\mathcal{H} = H(t) + \mathcal{H}_B + \mathcal{W} \tag{15}$$

Because $\mathcal{H}$ is assumed to be a single-particle Hamiltonian, the dynamics of the single-particle reduced density matrix is given by

$$\frac{d\tilde{\rho}}{dt} = -\frac{i}{\hbar}[\mathcal{H}, \tilde{\rho}] \tag{16}$$

where $\tilde{\rho}$ is the density matrix for the tripartite system.

We now show that the simple equations of motion arise naturally for the tripartite system in eq 15 provided that (1) only the explicit lead levels couple to the Fermionic reservoir, (2) all explicit lead levels are damped identically and are not coupled among each other via the reservoir, (3) the bandwidth of the Fermionic reservoir is the largest energy scale in the problem such that the WBL applies, (4) the relaxation dynamics of the explicit lead levels is independent of the presence of the

dx.doi.org/10.1021/jp505771f | J. Phys. Chem. C 2014, 118, 20009−20017

molecule, and (5) any time-dependence in the leads (for instance, a time-dependent bias voltage) can be considered adiabatically. The validity of the approximations has been exemplified in Sections 3.1 and 3.2.

The desired equation of motion for $\rho = (P + Q)\tilde{\rho}(P + Q)$ is obtained by projecting eq 16 onto the Hilbert space used in the simulations:

$$\begin{aligned}\frac{\mathrm{d}\rho}{\mathrm{d}t} &= -\frac{\mathrm{i}}{\hbar}(P + Q)(\mathcal{H}\tilde{\rho} - \tilde{\rho}\mathcal{H})(P + Q)\\ &= -\frac{\mathrm{i}}{\hbar}(P + Q)(\mathcal{H}(P + Q + B)(P + Q + B)\tilde{\rho}\\ &\quad - \tilde{\rho}(P + Q + B)(P + Q + B)\mathcal{H})(P + Q)\\ &= -\frac{\mathrm{i}}{\hbar}[H, \rho] - \frac{\mathrm{i}}{\hbar}(\mathcal{W}B\tilde{\rho}(P + Q) - (P + Q)\tilde{\rho}B\mathcal{W})\end{aligned} \tag{17}$$

where the operator B projects onto reservoir states; $(P + Q + B)$ is the identity and $\mathcal{W} = (P + Q)\mathcal{H}B + B\mathcal{H}(P + Q) = Q\mathcal{H}B + B\mathcal{H}Q$, where we have supposed that only the explicit lead levels are coupled to the reservoir via $\mathcal{W}$. We also used the fact that $H = (P + Q)\mathcal{H}(P + Q)$ and the orthogonality between the different projection operators, i.e., $PQ = PB = QB = 0$. Such orthogonality between the projection operators requires using basis states for the molecular and lead regions that are orthogonal among each other. The first part of eq 17 corresponds to the unitary dynamics of the junction, while the second part captures electron injection and decay processes.

The density matrix elements of $B\tilde{\rho}(P + Q)$ and $(P + Q)\tilde{\rho}B$ all have one index in the reservoir and one in the junction. To obtain a closed equation within the junction we must break these terms apart. To this end, we employ the NEGF formulation and apply the Dyson equation on the Keldysh contour to the second part of eq 17.

First, we identify the lesser Green's function in terms of the single-particle reduced density matrix of the tripartite system as

$$\tilde{\rho}_{ji}(t) = -\mathrm{i}G^{<}_{ji}(t, t) = \langle c_i^{\dagger}(t)c_j(t)\rangle \tag{18}$$

In terms of $G^{<}_{ji}(t,t)$ the junction-reservoir coupling terms in the dynamics are given by

$$\begin{aligned}&-\frac{\mathrm{i}}{\hbar}(\mathcal{W}B\tilde{\rho}(P + Q) - (P + Q)\tilde{\rho}B\mathcal{W})\\ &= -\frac{1}{\hbar}(\mathcal{W}BG^{<}(t, t)(P + Q) - (P + Q)G^{<}(t, t)B\mathcal{W})\\ &= -\frac{1}{\hbar}\sum_b (\mathcal{W}_{qb}G^{<}_{bk}(t, t) - G^{<}_{kb}(t, t)\mathcal{W}_{bq})\end{aligned} \tag{19}$$

In writing the last term in eq 19, explicit indexes have been used to highlight the terms that contribute to the dynamics of the density matrix. Here, and throughout, the b index runs over the reservoir levels, q over the explicit lead levels, and k over junction levels. Note, however, that tensor notation has been adopted and that the two contributing terms enter into different submatrices in the dynamics of the density matrix. Next we write the Hamiltonian as $\mathcal{H} = (H(t) + \mathcal{H}_B) + \mathcal{W}$, where $\mathcal{W}$ is considered as a perturbation to the uncoupled junction plus reservoir system, apply the Dyson equation to the Green's function ordered on the Keldysh contour, and use the Langreth rules to obtain the lesser Green's function:

$$\begin{aligned}G^{<}_{bk}(t, t) &= \int \mathrm{d}\tau G^{(0),\mathrm{ret}}_{bb}(t, \tau)\mathcal{W}_{bq}G^{<}_{qk}(\tau, t)\\ &\quad + \int \mathrm{d}\tau G^{(0),<}_{bb}(t, \tau)\mathcal{W}_{bq}G^{\mathrm{adv}}_{qk}(\tau, t)\end{aligned} \tag{20}$$

$$\begin{aligned}G^{<}_{kb}(t, t) &= \int \mathrm{d}\tau G^{\mathrm{ret}}_{kq}(t, \tau)\mathcal{W}_{qb}G^{(0),<}_{bb}(\tau, t)\\ &\quad + \int \mathrm{d}\tau G^{<}_{kq}(t, \tau)\mathcal{W}_{qb}G^{(0),\mathrm{adv}}_{bb}(\tau, t)\end{aligned} \tag{21}$$

Here the (0) superscript denotes the uncoupled Green's functions of the junction plus reservoir. In general, eqs 20 and 21 require a sum over q. We assume, however, that the reservoir does not mix the lead levels. Effectively, this requires supposing that the specific q label in the $\mathcal{W}_{bq}$ couplings in eq 19 is the same as the one in eqs 20 and 21. Inserting eqs 20 and 21 into eq 19, we shall obtain a closed equation for ρ. The resulting equation is reminiscent of eq 16.9 in ref 43 without the final term, which handles the initial state. Note, however, that the partition used in ref 43 does not consider an explicit segment of the lead as part of the system; hence, the spirit and range of validity of the equations is fundamentally different. Further note that we do not consider the vertical contour piece attached to the Keldysh contour that leads to initial time dependence in order to keep the equations local in time.

The terms containing a coupled lesser Green's function in eqs 20 and 21 comprise the decay terms. We can write them as

$$\int \mathrm{d}\tau G^{<}_{kq}(t, \tau)\Sigma^{(0),\mathrm{adv}}_{qq}(\tau, t) - \int \mathrm{d}\tau \Sigma^{(0),\mathrm{ret}}_{qq}(t, \tau)G^{<}_{qk}(\tau, t) \tag{22}$$

where expressions of the form $\Sigma^{(0),\mathrm{adv}}_{qq}(\tau, t) = \Sigma_b \mathcal{W}_{qb}G^{(0),\mathrm{adv}}_{bb}(\tau, t)\mathcal{W}_{bq}$ are self-energies. Applying the WBL to the junction−reservoir coupling, and assuming that all lead states are damped equally, we have

$$\Sigma^{(0),\mathrm{adv}}_{qq}(\tau, t) = \frac{i}{2}\gamma\delta(\tau - t) \tag{23}$$

$$\Sigma^{(0),\mathrm{ret}}_{qq}(t, \tau) = -\frac{\mathrm{i}}{2}\gamma\delta(t - \tau) \tag{24}$$

where $\gamma \simeq \gamma_{qq}(\omega) = 2\pi\sum_b \mathcal{W}_{qb}\delta(\varepsilon_b - \hbar\omega)\mathcal{W}_{bq}$.[43] Performing the time integrations, we have

$$\frac{\mathrm{i}}{2}\gamma G^{<}_{kq}(t, t) + \frac{\mathrm{i}}{2}\gamma G^{<}_{qk}(t, t) = -\frac{1}{2}\gamma(\rho_{kq} + \rho_{qk}) \tag{25}$$

where the index k runs over the entire junction. When restricted to the explicit leads, the two terms are identical and we obtain $-\gamma Q\rho Q$. When k runs over the molecular states, we have two hermitian conjugate terms, $-1/2\gamma(Q\rho P + P\rho Q)$. Note that, in essence, in the WBL the decay terms introduced by the Fermionic reservoir can be captured by an imaginary potential. This is consistent with previous observations in semi-infinite tight-binding chains[29] and provides the physical basis to the introduction of imaginary potentials in ref 25. When the Fermionic reservoir cannot be described in the WBL, non-Markovian effects can play an important role in the dynamics.[44,45]

The terms in eqs 20 and 21 containing an uncoupled lesser Green's function comprise the injection term. We can write them as

$$\gamma Z = \int \mathrm{d}\tau G^{\mathrm{ret}}_{kq}(t,\tau)\Sigma^{(0),<}_{qq}(\tau,t) - \int \mathrm{d}\tau \Sigma^{(0),<}_{qq}(t,\tau)G^{\mathrm{adv}}_{qk}(\tau,t) \tag{26}$$

Assuming that the junction-reservoir couplings and the reservoir Hamiltonian are time-independent, applying the WBL to the junction-reservoir coupling, and assuming that all lead states are damped equally, we can evaluate the self-energies

$$\Sigma^{(0),<}_{qq}(\tau,t) = \sum_b \mathcal{W}_{qb}G^{(0),<}_{bb}(\tau,t)\mathcal{W}_{bq} \tag{27}$$

$$= \int \frac{\mathrm{d}\omega}{2\pi}\mathrm{e}^{-\mathrm{i}\omega(\tau-t)}\mathrm{i}f(\omega)\gamma \tag{28}$$

where $f(\omega)$ is the Fermi distribution of the leads.[43] Inserting above, we have

$$\gamma Z = \int \mathrm{d}\tau \int \frac{\mathrm{d}\omega}{2\pi}\mathrm{e}^{-\mathrm{i}\omega(\tau-t)}\mathrm{i}f(\omega)\gamma G^{\mathrm{ret}}_{kq}(t,\tau) - \int \mathrm{d}\tau \int \frac{\mathrm{d}\omega}{2\pi}\mathrm{e}^{-\mathrm{i}\omega(t-\tau)}\mathrm{i}f(\omega)\gamma G^{\mathrm{adv}}_{qk}(\tau,t) \tag{29}$$

$$= \gamma \int \frac{\mathrm{d}\omega}{2\pi}f(\omega)i\int \mathrm{d}\tau[\mathrm{e}^{-\mathrm{i}\omega(\tau-t)}G^{\mathrm{ret}}(t,\tau)Q - \mathrm{e}^{-\mathrm{i}\omega(t-\tau)}QG^{\mathrm{adv}}(\tau,t)] \tag{30}$$

$$= \gamma \int \frac{d\omega}{2\pi}f(\omega)\tilde{A}(\omega,t) \tag{31}$$

where the last line defines the auxiliary function

$$\tilde{A}(\omega,t) = \mathrm{i}\int \mathrm{d}\tau[\mathrm{e}^{-\mathrm{i}\omega(\tau-t)}G^{\mathrm{ret}}(t,\tau)Q - \mathrm{e}^{-\mathrm{i}\omega(t-\tau)}QG^{\mathrm{adv}}(\tau,t)] \tag{32}$$

The term γZ represents the relaxation of charges in the explicit leads. To lowest order, this dynamics is expected to be independent of the presence of the molecule. Thus, in the following we shall consider the Green's functions to lowest-zeroth order in the molecule–lead coupling. Under this assumption, the Green's functions commute with Q, and we have $\tilde{A}(\omega,t) = Q\tilde{A}(\omega,t)Q$. Considering the explicit lead Hamiltonian H_{L} in eq 1 to be independent of time, the Green's functions become dependent only on the time difference and we can introduce the Fourier components. As a consequence, the dependence on time t drops out, and $\tilde{A}(\omega,t)$ equals the spectral function.

$$\tilde{A}(\omega) = \mathrm{i}(G^{\mathrm{ret}}(\omega) - G^{\mathrm{adv}}(\omega)) = A(\omega) \tag{33}$$

In conclusion, we have

$$\gamma Z = \gamma \int \frac{\mathrm{d}\omega}{2\pi}f(\omega)A(\omega) = \gamma\rho^{eq} \tag{34}$$

A time-dependent bias can be introduced via a time-dependent chemical potential in the Fermi function. This relies on the adiabatic assumption that the leads remain in equilibrium at all times. That is

$$\gamma Z(t) = \gamma \int \frac{\mathrm{d}\omega}{2\pi}f(\omega,t)A(\omega) = \gamma\rho^{eq}(t) \tag{35}$$

Collecting terms, we arrive at

$$\dot{\rho} = -\frac{\mathrm{i}}{\hbar}[H,\rho] - \frac{\gamma}{\hbar}Q(\rho-\rho^{eq})Q - \frac{\gamma}{2\hbar}(Q\rho P + P\rho Q) \tag{36}$$

which is exactly the same as eq 8.

The dynamics of the single-particle reduced density matrix for the full junction–bath system, $\tilde{\rho}(t)$, preserves positivity because it is governed by the Liouville equation. The reduced density matrix of the junction, $\rho(t)$, obtained by projection constitutes a principal submatrix of a hermitian, positive semidefinite matrix and is thus also positive semidefinite. Consequently, the exact reduced dynamics, using eq 31 as the injections term, preserves positivity. Explicit proof, as to whether the final perturbative approximation, $\tilde{A}(\omega,t) \simeq Q\tilde{A}(\omega,t)Q$, conserves positivity exactly or only asymptotically remains outstanding.

4. CONCLUSIONS

We have introduced a simple method to model time-dependent transport along metal–molecule–metal junctions in which the metallic contacts are modeled explicitly as a discrete set of levels that are dynamically broadened via damping terms in the equations of motion. Through an explicit derivation of the underlying equations of motion eq 8 in the context of NEGFs, the method is shown to apply to junctions that can be described by an effective independent particle Hamiltonian (such as those generated by TDDFT) with arbitrary time-dependent driving forces acting on the molecule. The method further allows for arbitrary temperature and molecule–lead coupling strengths and time-dependent changes in the applied voltage that do not generate excitations in the leads. The resulting set of equations are intuitively clear and trivial to computationally implement and parallelize.

The damping terms in the dynamics arise because of coupling of the explicit lead levels to a larger Fermionic reservoir. The simple form in eq 8 emerges in the limiting case where it is assumed that (i) the Fermionic reservoir couples identically and independently with each explicit lead level, (ii) the WBL applies to the Fermionic reservoir, and (iii) the relaxation dynamics of the explicit lead levels is independent of the presence of the molecule.

By contrasting with a state-of-the-art NEGF method, the simple method was shown to have a well-defined range where results are independent of artificial modeling parameters and to quantitatively reproduce asymptotic and transient transport results for model molecular junctions driven by applied voltages and laser fields. Specifically, it was shown that accurate results emerge when the damping term induced by γ in eq 8 and the level spacing $\Delta\varepsilon_q$ between the explicit lead levels are chosen such that $\Gamma > \gamma \geq \Delta\varepsilon_q/2$, where Γ is the effective molecule–lead coupling defined in eq 5. Under these conditions, the discrete set of levels in the leads effectively behave as a continuum structure and the dynamics captures all relevant Γ-induced processes before the γ-induced relaxation is dominant. Furthermore, the method was shown to correctly capture the molecular phase determining the phase lag of a coherent control map. Such molecular phase is known to sensitively depend on the continuum structure; hence, this is a strong indication that the broadening procedure in eq 8 reproduces such structure correctly. The method is also expected to be adaptable to situations beyond the wide band limit where the energy structure of the leads and the energy dependence of the molecule–lead couplings are of relevance.

Nevertheless, the method is expected to be less computationally efficient than NEGF methods where the effects of the leads are captured implicitly. This is particularly true in the weak-coupling limit where a fine energy grid is required to achieve a range where the results are independent of the fictitious modeling parameters.

dx.doi.org/10.1021/jp505771f | J. Phys. Chem. C 2014, 118, 20009–20017

AUTHOR INFORMATION

Corresponding Author

*E-mail: ignacio.franco@rochester.edu.

Notes

The authors declare no competing financial interest.

ACKNOWLEDGMENTS

This work was supported by University of Rochester startup funds. T.H. thanks the Lundbeck Foundation and the Swedish Research Council (VR). The authors thank Prof. Joseph E. Subotnik for useful discussions and Prof. GuanHua Chen, Mr. SiuKong Koo, and Mr. Yu Zhang for providing a copy of the software Lodestar that was used to generate the NEGF time-dependent transport results. L.C. thanks Dr. Linjun Wang for helpful discussions.

REFERENCES

(1) Nitzan, A. Electron Transmission through Molecules and Molecular Interfaces. *Annu. Rev. Phys. Chem.* **2001**, *52*, 681−750.

(2) Datta, S. *Quantum Transport: Atom to Transistor*; Cambridge University Press: New York, 2005.

(3) Di Ventra, M. *Electrical Transport in Nanoscale System*; Cambridge University Press: New York, 2008.

(4) Bergfield, J. P.; Ratner, M. A. Forty Years of Molecular Electronics: Non-Equilibrium Heat and Charge Transport at the Nanoscale. *Phys. Status Solidi B* **2013**, *250*, 2249−2266.

(5) Meir, Y.; Wingreen, N. S. Landauer Formula for the Current through an Interacting Electron Region. *Phys. Rev. Lett.* **1992**, *68*, 2512−2515.

(6) Herrmann, C.; Solomon, G. C.; Subotnik, J. E.; Mujica, V.; Ratner, M. A. Ghost Transmission: How Large Basis Sets Can Make Electron Transport Calculations Worse. *J. Chem. Phys.* **2010**, *132*, 024103.

(7) Jauho, A.-P.; Wingreen, N. S.; Meir, Y. Time-Dependent Transport in Interacting and Noninteracting Resonant-Tunneling Systems. *Phys. Rev. B* **1994**, *50*, 5528−5544.

(8) Kurth, S.; Stefanucci, G.; Almbladh, C.-O.; Rubio, A.; Gross, E. K. U. Time-Dependent Quantum Transport: A Practical Scheme Using Density Functional Theory. *Phys. Rev. B* **2005**, *72*, 035308.

(9) Kohler, S.; Lehmann, J.; Hänggi, P. Driven Quantum Transport on the Nanoscale. *Phys. Rep.* **2005**, *406*, 379−443.

(10) Zheng, X.; Wang, F.; Yam, C. Y.; Mo, Y.; Chen, G. H. Time-Dependent Density-Functional Theory for Open Systems. *Phys. Rev. B* **2007**, *75*, 195127.

(11) Myöhänen, P.; Stan, A.; Stefanucci, G.; van Leeuwen, R. Kadanoff-Baym Approach to Quantum Transport through Interacting Nanoscale Systems: From the Transient to the Steady-State Regime. *Phys. Rev. B* **2009**, *80*, 115107.

(12) Croy, A.; Saalmann, U. Propagation Scheme for Nonequilibrium Dynamics of Electron Transport in Nanoscale Devices. *Phys. Rev. B* **2009**, *80*, 245311.

(13) Zheng, X.; Chen, G. H.; Mo, Y.; Koo, S.; Tian, H.; Yam, C.; Yan, Y. Time-Dependent Density Functional Theory for Quantum Transport. *J. Chem. Phys.* **2010**, *133*, 114101.

(14) Xie, H.; Jiang, F.; Tian, H.; Zheng, X.; Kwok, Y.; Chen, S.; Yam, C.; Yan, Y.; Chen, G. H. Time-Dependent Quantum Transport: An Efficient Method Based on Liouville-von-Neumann Equation for Single-Electron Density Matrix. *J. Chem. Phys.* **2012**, *137*, 044113.

(15) Zhang, Y.; Chen, S.; Chen, G. H. First-Principles Time-Dependent Quantum Transport Theory. *Phys. Rev. B* **2013**, *87*, 085110.

(16) Welack, S.; Schreiber, M.; Kleinekathöfer, U. The Influence of Ultrafast Laser Pulses on Electron Transfer in Molecular Wires Studied by a Non-Markovian Density-Matrix Approach. *J. Chem. Phys.* **2006**, *124*, 044712.

(17) May, V.; Kühn, O. Optical Field Control of Charge Transmission through a Molecular Wire. I. Generalized Master Equation Description. *Phys. Rev. B* **2008**, *77*, 115439.

(18) Tikhonov, A.; Coalson, R. D.; Dahnovsky, Y. Calculating Electron Transport in a Tight Binding Model of a Field-Driven Molecular Wire: Floquet Theory Approach. *J. Chem. Phys.* **2002**, *116*, 10909−10920.

(19) Arrachea, L.; Moskalets, M. Relation Between Scattering-Matrix and Keldysh Formalisms for Quantum Transport Driven by Time-Periodic Fields. *Phys. Rev. B* **2006**, *74*, 245322.

(20) Wang, H.; Thoss, M. Multilayer Multiconfiguration Time-Dependent Hartree Study of Vibrationally Coupled Electron Transport Using the Scattering-State Representation. *J. Phys. Chem. A* **2013**, *117*, 7431−7441.

(21) Wang, H.; Thoss, M. Numerically Exact, Time-Dependent Study of Correlated Electron Transport in Model Molecular Junctions. *J. Chem. Phys.* **2013**, *138*, 134704.

(22) Sánchez, C. G.; Stamenova, M.; Sanvito, S.; Bowler, D. R.; Horsfield, A. P.; Todorov, T. N. Molecular Conduction: Do Time-Dependent Simulations Tell You More Than the Landauer Approach? *J. Chem. Phys.* **2006**, *124*, 214708.

(23) Subotnik, J. E.; Hansen, T.; Ratner, M. A.; Nitzan, A. Nonequilibrium Steady State Transport via the Reduced Density Matrix Operator. *J. Chem. Phys.* **2009**, *130*, 144105.

(24) Ajisaka, S.; Barra, F.; Mejía-Monasterio, C.; Prosen, T. Current in Coherent Quantum Systems Connected to Mesoscopic Fermi Reservoirs. *Phys. Scr.* **2012**, *86*, 058501.

(25) Zelovich, T.; Kronik, L.; Hod, O. State Representation Approach for Atomistic Time-Dependent Transport Calculations in Molecular Junctions. *J. Chem. Theor. Comp.* **2014**, 10.1021/ct500135e, in press.

(26) Galperin, M.; Nitzan, A. Molecular Optoelectronics: The Interaction of Molecular Conduction Junctions with Light. *Phys. Chem. Chem. Phys.* **2012**, *14*, 9421−9438.

(27) Shapiro, M.; Brumer, P. *Quantum Control of Molecular Processes*; WILEY-VCH: Weinheim, Ger., 2012.

(28) Franco, I.; Brumer, P. Minimum Requirements for Laser-Induced Symmetry Breaking in Quantum and Classical Mechanics. *J. Phys. B: At., Mol. Opt. Phys.* **2008**, *41*, 074003.

(29) Franco, I.; Shapiro, M.; Brumer, P. Laser-Induced Currents along Molecular Wire Junctions. *J. Chem. Phys.* **2008**, *128*, 244906.

(30) Franco, I.; Shapiro, M.; Brumer, P. Robust Ultrafast Currents in Molecular Wires through Stark Shifts. *Phys. Rev. Lett.* **2007**, *99*, 126802.

(31) Lehmann, J.; Kohler, S.; May, V.; Hänggi, P. Vibrational Effects in Laser-Driven Molecular Wires. *J. Chem. Phys.* **2004**, *121*, 2278−2288.

(32) Lehmann, J.; Kohler, S.; Hänggi, P.; Nitzan, A. Rectification of Laser-Induced Electronic Transport through Molecules. *J. Chem. Phys.* **2003**, *118*, 3283−3293.

(33) Grossmann, F.; Dittrich, T.; Jung, P.; Hänggi, P. Coherent Destruction of Tunneling. *Phys. Rev. Lett.* **1991**, *67*, 516−519.

(34) Lehmann, J.; Camalet, S.; Kohler, S.; Hänggi, P. Laser Controlled Molecular Switches and Transistors. *Chem. Phys. Lett.* **2003**, *368*, 282−288.

(35) Kleinekathöfer, U.; Li, G.; Welack, S.; Schreiber, M. Switching the Current through Model Molecular Wires with Gaussian Laser Pulses. *Europhys. Lett.* **2006**, *75*, 139−145.

(36) Grossmann, F.; Hänggi, P. Localization in a Driven Two-Level Dynamics. *Europhys. Lett.* **1992**, *18*, 571−576.

(37) Xie, H.; Kwok, Y.; Zhang, Y.; Jiang, F.; Zheng, X.; Yan, Y.; Chen, G. H. Time-Dependent Quantum Transport Theory and its Applications to Graphene Nanoribbons. *Phys. Status Solidi B* **2013**, *250*, 2481−2494.

(38) Hu, J.; Luo, M.; Jiang, F.; Xu, R.-X.; Yan, Y. Padé Spectrum Decompositions of Quantum Distribution Functions and Optimal Hierarchical Equations of Motion Construction for Quantum Open Systems. *J. Chem. Phys.* **2011**, *134*, 244106.

(39) Kohler, S.; Camalet, S.; Strass, M.; Lehmann, J.; Ingold, G.-L.; Hänggi, P. Charge Transport through a Molecule Driven by a High-Frequency Field. *Chem. Phys.* **2004**, *296*, 243−249.

(40) Gordon, R. J.; Zhu, L.; Seideman, T. Coherent Control of Chemical Reactions. *Acc. Chem. Res.* **1999**, *32*, 1007−1016.

(41) Lefebvre-Brion, H.; Seideman, T.; Gordon, R. J. Multichannel Quantum Defect Calculation of the Phase Lag in the Coherent Control of HI. *J. Chem. Phys.* **2001**, *114*, 9402−9407.

(42) Note that the Floquet theory results reported in ref 31 exhibit a shift in the molecular phase with respect to the exact NEGF values.
(43) Stefanucci, G.; van Leeuwen, R. *Nonequilibrium Many-Body Theory of Quantum Systems: A Modern Introduction*; Cambridge University Press: New York, 2013.
(44) Kolesov, G.; Dahnovsky, Y. Correlated Electron Dynamics in Quantum-Qot Sensitized Solar Cell: Kadanoff-Baym versus Markovian Approach. *Phys. Rev. B* **2012**, *85*, 241309.
(45) Tian, H.; Chen, G. H. An Efficient Solution of Liouville-von Neumann Equation That Is Applicable to Zero and Finite Temperatures. *J. Chem. Phys.* **2012**, *137*, 204114.